Coherent Phase Modulation Transfer in Counter-Propagating Parametric Down-Conversion

C. Stromqvist, V. Pasiskevicius, Carlota Canalias, Carlos Montes

Coherent Phase Modulation Transfer in Counter-Propagating Parametric Down-Conversion

G. Strömqvist,[1] V. Pasiskevicius,[1] C. Canalias,[1] and C. Montes[2]

[1]*Department of Applied Physics, KTH,*
Roslagstullbacken 21, 10691 Stockholm, Sweden
[2]*LPMC-CNRS, Université de Nice - Sophia Antipolis,*
Parc Valrose, F-06108 Nice, France

(Dated: May 9, 2011)

Abstract

Distributed positive feedback established by a counter-propagating three-wave mixing process in a sub-micrometer structured second-order nonlinear medium leads to mirrorless parametric oscillation with unusual spectral properties. In this work, we demonstrate experimentally and theoretically that the phase modulation of the pump is coherently transferred to the co-propagating parametric wave, while the counter-propagating wave retains a narrow bandwidth and high coherence. The main mechanisms responsible for these properties are the maximized convective separation between the counter-propagating waves, as well as the associated phase-locking between the pump and the co-propagating parametric wave. This suggests that mirrorless optical parametric oscillators can be pumped with incoherent light and still generate highly coherent backward-propagating radiation.

PACS numbers: 42.65.Lm, 42.65.Yj, 78.67.Pt, 42.70.Mp

The lowest-order nonlinear interactions, collectively called three-wave mixing (TWM), are important in many different physical contexts, e.g. interactions in plasma [1, 2], hydrodynamics and internal gravity waves [3], planetary Rossby waves which are related to the global climate [4], interactions of bulk and surface acoustic waves [5, 6], matter waves [7] and, indeed, in nonlinear optics [8]. Optical parametric amplification (OPA) of lower frequency waves in a TWM process where photons $\hbar\omega_p$ of the wave of the highest frequency, the pump, are split into two photons of lower energy, the signal $\hbar\omega_s$ and the idler $\hbar\omega_i$, such that the energy conservation, $\omega_p = \omega_s + \omega_i$, and the momentum conservation, $\mathbf{k_p} = \mathbf{k_s} + \mathbf{k_i}$, conditions are satisfied, has large practical importance for the generation of high-energy ultrashort pulses in attosecond systems [9], as well as in quantum optics experiments for entangled photon-pair generation [10] and generation of squeezed vacuum states [11].

The coherence properties of the waves generated in the TWM down-conversion process have been subject of investigation from the very beginning of nonlinear optics [12, 13]. For instance, from simple quantum optical considerations it was shown [12] that OPA behaves like a perfect phase-sensitive amplifier, where the output photon number and phase variances of the amplified signal wave faithfully represent the input variances within the uncertainty principle. It is a general property of TWM that the total interaction phase is fixed. In the case of a down-conversion process, the phases ϕ_j (where $j = p, s, i$) satisfy the relation:

$$\phi_p - \phi_s - \phi_i = \pi/2. \tag{1}$$

This feature has been utilized in passive all-optical carrier-envelope phase stabilization schemes [14]. In an optical parametric generation (OPG) process, which, by definition, is seeded by zero-point fluctuations and thermal background radiation, the phases of the individual signal or idler waves remain to a large extent random, although the pairwise correlation between the signal and idler waves does exist [15]. As a consequence, the signal and the idler waves generated in background-noise seeded singly-resonant optical parametric oscillators (OPOs) can, in general, be considered incoherent and their spectral widths are much larger than that of the pump wave, unless phase-sensitive filtering is artificially imposed [16]. The spectral width of the parametric gain is determined primarily by the dispersion of the nonlinear medium and it is maximized when the group velocity dispersion is zero, $\partial^2 k / \partial \omega^2 = 0$, at the degeneracy point ($\omega_s \backsimeq \omega_i$). Away from degeneracy, the convection operators in the coupled wave equations, $\mathbf{v_{g,j}} \cdot \nabla$, where $\mathbf{v_{g,j}}$ are the respective group

velocities, determine the spectral widths of the signal and the idler waves. Several scenarios leading to increased coherence of the generated parametric waves by exploiting convective wave separation have been theoretically investigated [17, 18].

In this work, we demonstrate experimentally and numerically that in a mirrorless optical parametric oscillator (MOPO), the device which relies on counter-propagating TWM for establishing a distributed positive feedback for sustained oscillation above threshold [19], the convective wave separation is maximized and responsible for the unusual spectral and coherence properties of the generated signal and idler waves. Specifically, this physical mechanism ensures that the frequency bandwidth of the backward-propagating idler will be narrow compared to that of the signal when a broadband pump is used. Moreover, as a consequence of the phase relation in Eq. (1), the phase modulation of the pump is then effectively transferred to the co-propagating parametric wave.

Proposed in 1966 [20], the first experimental demonstration of a MOPO was reported in 2007 [21]. The major difficulty in achieving mirrorless parametric oscillation is associated with satisfying the momentum conservation condition, which in scalar form reads $k_p = k_s - k_i$. In homogeneous dielectrics, the phase matching condition can possibly be satisfied only for large signal-idler detunings, with the signal frequency close to that of the pump and the idler frequency in the THz region. However, due to the very different diffraction properties of the near-infrared signal and the far-infrared idler, achieving oscillation in homogeneous dielectrics is problematic. By employing ferroelectric nonlinear crystals structured with sub-micrometer periodicity, Λ, quasi-phase matching (QPM) [8]

$$\Delta k = k_p - k_s + k_i = 2\pi/\Lambda, \tag{2}$$

can be utilized to achieve MOPO with counter-propagating idler k_i in the mid-infrared spectral range. In the experimental investigation of the spectral properties of a MOPO, we here employ a 6.5 mm-long periodically-poled $KTiOPO_4$ (PPKTP) crystal with a QPM period of $\Lambda = 800$ nm to convert the pump around 813.5 nm into a co-propagating signal at 1123.0 nm and a counter-propagating idler at 2952.2 nm. The crystal fabrication details have been reported elsewhere [21, 22].

From the momentum conservation condition in the TWM with counter-propagating idler (Eq. 2), one can derive and estimate the frequency variation in the counter-propagating

wave, $\Delta\omega_i$, as function of the frequency variation in the pump, $\Delta\omega_p$:

$$\Delta\omega_i = \Delta\omega_p \frac{v_{g,i}\,(v_{g,p} - v_{g,s})}{v_{g,p}\,(v_{g,i} + v_{g,s})}. \tag{3}$$

The sum of the group velocities in the denominator of Eq. 3, which is the result of the counter-propagating geometry, ensures that the frequency of the back-propagating wave is not sensitive to changes in the pump frequency. This also means that the bandwidth of the counter-propagating wave is much smaller than that of the pump and it should reach minimum in a special case when the group velocities of the pump and the co-propagating signal wave are equal. In this limit when $\Delta\omega_i/\Delta\omega_p \to 0$, the temporal phase of the counter-propagating idler wave is $\phi_i \backsimeq const.$ Then from Eq. 1, it follows that the partial derivatives of the co-propagating signal and pump phases with respect to time are approximately equal, $\partial_t\phi_s(t) \backsimeq \partial_t\phi_p(t)$. These are indeed very unusual properties for parametric oscillation. In a process which is seeded by random noise, the interaction establishes a counter-propagating wave with a coherence time much longer than both the seeding noise and the coherence time of the pump. At the same time, the phase of this counter-propagating wave acts as a stable phase reference, thereby forcing the phases of the pump and the co-propagating signal wave to lock and vary in synchronism. It should be stressed that Eq. 3 is only an estimate, because the actual spectra of the generated waves also depend on the details of the TWM dynamics. A numerical solution of the coupled wave equations will show that the above reasoning regarding the phases of the waves is qualitatively correct.

For the experimental verification of the convective phase locking in MOPOs, the above-mentioned PPKTP crystal was pumped with pulses centered at 814.5 nm with a frequency bandwidth of 1.21 THz. The pulse was stretched in a normal-dispersion stretcher and amplified in a Ti:Sapphire regenerative amplifier. The FWHM length of the amplified pulse was 480 ps and it was used for MOPO pumping. A small portion of the pump pulse was recompressed to close to transform-limited duration of 1 ps and was used as a reference for cross-correlation measurements. The MOPO reached threshold at the pump intensity of 0.8 GW/cm^2. The measured pump spectra (spectrometer Ando AQ-6315A, resolution 0.05 nm) at 1.3-times the threshold intensity are shown in Fig. 1(a), where the undepleted pump spectrum was measured when the pump beam propagated outside the structured area of the PPKTP and the MOPO was not operational. The linear frequency chirp of the pump, measured using cross-correlation with the reference pulse, was $d\omega_p/dt = 15.7$ mrad/ps^2.

This linear chirp provides a direct frequency-to-time mapping, implying that the spectral measurements also contain temporal information about the MOPO dynamics. By comparing the spectra in Fig. 1(a), we can see that, at this pump intensity, the MOPO starts oscillating after a delay of about 260 ps, corresponding to the difference in time between the beginning of the pulse (816.1 nm) and where the pump starts being depleted (814.7 nm). After the start of the MOPO oscillation, the pump is rapidly depleted and the depletion level of about 60% remains approximately constant until the end of the pump pulse. This shows that the counter-propagating TWM process indeed is very efficient. The measured spectrum of the MOPO signal had a central wavelength of 1123.0 nm and a FWMH spectral width of 410 GHz, as illustrated in Fig. 1(b). Cross-correlation measurements revealed that the pulse had a FWHM length of 160 ps, containing a positive linear frequency chirp of 16.0 mrad/ps^2. This value is close to the chirp of the pump, as expected if the picture of convective phase-locking and phase modulation transfer between pump and signal is correct. The measured idler spectrum (spectrometer Jobin Yvon iHR550, 0.55 nm resolution) shown in Fig. 1(c) reveals that the FWHM bandwidth is 23 GHz. Taking into account that the resolution of the spectrometer is limited to 19 GHz at 2.952 μm and assuming a Gaussian spectral shape, the deconvoluted idler frequency bandwidth is then about 13 GHz. Within the resolution of our measurements, the idler bandwidth did not depend on the amount or sign of chirp imposed on the pump wave. This was checked by passing the pump pulse through a delay line with anomalous group-delay dispersion so that the pump pulse with the same spectrum as in Fig. 1(a) had an opposite frequency chirp and a different pulse length.

As a final experiment, we investigated the compressibility of the signal pulse. If the linear frequency chirp is transferred from the pump to the co-propagating signal, the MOPO signal pulse should be compressible. To test this, we built a compressor with anomalous group-delay dispersion involving 4 bounces off a 1200 l/mm diffraction grating. The MOPO was pumped with positively chirped pulses of similar spectral and temporal widths as in the previous experiment. The signal pulse before and after the compressor was characterized using cross-correlation with the 1 ps-long reference pulse at the pump wavelength. The cross-correlation traces measured by employing noncollinear sum-frequency mixing in a 200 μm-long BBO crystal are shown in Fig. 2 for different compressor lengths. The compressibility of the MOPO signal proves that the phase modulation which is imposed on the pump pulse is transferred to the signal. This is a unique feature of the MOPO, enabled by the counter-

propagating TWM process.

The transfer of phase modulation from the pump to the signal can also be shown theoretically. In order to elucidate the unusual coherence properties in the MOPO and also to model the experimental situation, we numerically solved the coupled wave equations using the slowly varying envelope and plane wave approximations for parametric down-conversion in counter-propagating geometry:

$$(\partial_t + v_{g,p}\partial_z + \gamma_p + i\beta_p\partial_{tt})\,\mathbf{A_p} = -\sigma_p \mathbf{A_s}\mathbf{A_i}, \tag{4a}$$

$$(\partial_t + v_{g,s}\partial_z + \gamma_s + i\beta_s\partial_{tt})\,\mathbf{A_s} = \sigma_s \mathbf{A_p}\mathbf{A_i^*}, \tag{4b}$$

$$(\partial_t - v_{g,i}\partial_z + \gamma_i + i\beta_i\partial_{tt})\,\mathbf{A_i} = \sigma_i \mathbf{A_p}\mathbf{A_s^*}. \tag{4c}$$

Here $\mathbf{A_j}$, β_j, γ_j, $\sigma_j = 2\pi d_{eff} v_{g,j}/(\lambda_j n_j)$ are the field amplitude, the group-velocity dispersion, the loss and the nonlinear coupling coefficients for the $j = p, s, i$ wave, respectively. A model PPKTP crystal with a length of 6.5 mm and an effective nonlinearity of $d_{eff} = 9$ pm/V was excited with an asymmetric super-Gaussian pump pulse with amplitude $\mathbf{A_p}(t) = \mathbf{A_{p0}}[1 - t/(2\Delta t_0)]\exp[i\phi_p(t) - ((t - t_0)/\Delta t_1)^8/2]$. The pulse was centered at $t_0 = 441$ ps and the temporal widths $\Delta t_0 = 1766$ ps and $\Delta t_1 = 220$ ps were chosen in order to fit the experimental intensity pump shape and to get a FWHM pulse length of $\Delta t_p = 400$ ps. The theoretical pump pulse contained a linear frequency chirp, given by the quadratic phase modulation $\phi_p(t) = \alpha_2((t - t_0)/\tau_0)^2$, where $\tau_0 = 2/(\sigma_p A_{p0})$ is the characteristic nonlinear interaction time, defining the characteristic nonlinear interaction length, $L_{nl} = v_{g,p}\tau_0$. For the pump intensity of 1.1 GW/cm^2, which is a pump intensity close to the experimental input, the characteristic parameter values are $\tau_0 = 6.9$ ps and $L_{nl} = 1$ mm. The pump chirp parameter $\alpha_2 = 0.46$ was chosen to give a positive chirp and a spectral width of 1.27 THz. The dispersion parameters for the KTP crystal were calculated using the Sellmeier expansion from Ref. [23] and the quasi-phase matched interaction generated signal and idler waves around around 1125 nm and 2952 nm, respectively, for a pump wavelength of 814.5 nm. For these central wavelengths, the spectral compression in the idler, as estimated from Eq. 3, is $\Delta\omega_i/\Delta\omega_p \backsimeq 1/92$.

Simulations of the MOPO at the pump intensity of 1.1 GW/cm^2 reveal that the oscillation develops after an initial delay of 300 ps and TWM starts depleting the trailing end of the pump pulse where the high-frequency components are located due to the chirp. This can be seen in the comparison between the input and output pump spectra in Fig. 3(a). Fig. 3(b)

and Fig. 3(c) show that the generated signal obtains a FWHM spectral width of 440 GHz, whereas that of the idler is only 6.5 GHz, i.e. about 200-times narrower than the initial pump spectrum and 70-times narrower than the signal. The strong asymmetry in the spectral widths of the signal and idler is related to the amount of phase modulation in the waves. This is illustrated in Fig. 4, where the phase of the idler wave shows very little variation along the crystal, while the phases of the signal and pump remain locked. Qualitatively one can understand this by realizing that the initial pulse front of the backward-propagating idler wave is rapidly separated from the signal and the pump, akin to fast convection, and seeds the parametric amplification process upstream, while maintaining its initial phase and enforcing the phase of the signal, owing to the phase relation in Eq. 1. Simulations of the MOPO pumped with a wave containing random phase modulation give qualitatively similar results, i.e. the convective phase locking mechanism ensures the generation of a narrowband coherent counter-propagating idler wave, while the signal inherits the random phase modulation from the pump.

In conclusion, we have employed a mirrorless OPO realized in a sub-micrometer periodically-poled KTP crystal for experimental demonstration that the phase of the pump wave is coherently transferred to the co-propagating OPO signal, as a result of the maximized convective separation of the pump and idler pulse fronts. This convective mechanism, as was elucidated by the numerical modeling, gives rise to a narrowband counter-propagating idler wave, regardless of the details of the pump phase.

This work has been supported by grants from the Swedish Research Council (VR), Knut and Alice Wallenberg foundation and Göran Gustafsson foundation. The authors acknowledge the GDR PhoNoMi2 no 3073 of the CNRS (Centre National de la Recherche Scientifique) devoted to Nonlinear Photonics in Microstructured Materials. The authors are thankful for useful discussions with Fredrik Laurell, Pierre Aschieri and Antonio Picozzi.

[1] A. Bers, D. J. Kaup and H. Reiman, Phys. Rev. Lett., **37**, 182, (1976)

[2] M. N. Rosenbluth, Phys. Rev. Lett., **29**, 565, (1972)

[3] F. P. Bretherton, J. Fluid Mech., **20**, 457, (1964)

[4] M. S. Longuet-Higgins and A. E. Gill, Proc. R. Soc. London A, **299**, 120, (1967)

[5] N. S. Shiren, Proc. IEEE, **53**, 1540, (1965)

[6] L. O. Svaasand, Appl. Phys. Lett., **15**, 300, (1969)

[7] H. Y. Ling, in *Coherence and quantum optics VIII*, edited by N. P. Bigelow, and J. H. Eberly, and C. R. Stroud, and A. Walmsley (Kluwer Academic Plenum, 2003), pp.573-574

[8] J. A. Armstrong, N. Bloembergen, J. Ducuing and P. S. Pershan, Phys. Rev., **127**, 1918, (1962)

[9] Z. Major, S. A. Trushin, I. Ahmad, M. Siebold, C. Wandt, S. Klingebiel, T. Wa, J. Flop, A. Henig, S. Kruber, R. Weingartner, A. Popp, J. Osterhoff, R. Hrlein, J. Hein, V. Pervak, A. Apolonski, F. Krausz and S. Karsch, Rev. Laser Eng., **37**, 431, (2009)

[10] T. Yamamoto, M. Koashi, S. K. Özdemir and N. Imoto, Nature, **421**, 343, (2003)

[11] L. A. Wu, H. J. Kimble, J. L. Hall and H. Wu, Phys. Rev. Lett., **57**, 2520, (1986)

[12] W. H. Louisell, A. Yariv and A. E. Siegman, Phys. Rev., **124**, 1646, (1961)

[13] R. J. Glauber, *Quantum theory of optical coherence*, (Wiley-VCH, 2007)

[14] A. Baltuska, T. Fuji and T. Kobayashi, Phys. Rev. Lett., **88**, 133901, (2002)

[15] B. Dayan, A. Peer, A. A. Friesem and Y. Silberberg, Phys. Rev. Lett., **93**, 023005, (2004)

[16] M. Henriksson, M. Tiihonen, V. Pasiskevicius and F. Laurell, Optics Lett., **31**, 1878, (2006)

[17] A. Picozzi and M. Hælterman, Phys. Rev. Lett., **86**, 2010, (2001)

[18] A. Picozzi, C. Montes and M. Hælterman, Phys. Rev. E, **66**, 056605-1-14, (2002)

[19] Y. J. Ding and J. B. Khurgin, IEEE J. Quantum Electron., **32**, 1574, (1996)

[20] S. E. Harris, Appl. Phys. Lett., **9**, 114, (1966)

[21] C. Canalias and V. Pasiskevicius, Nature Photonics, **1**, 459, (2007)

[22] C. Canalias, V. Pasiskevicius, R. Clemens and F. Laurell, Appl. Phys. Lett., **82**, 4233, (2003)

[23] K. Kato and E. Takaoka, Appl. Opt., **41**, 5040, (2002)

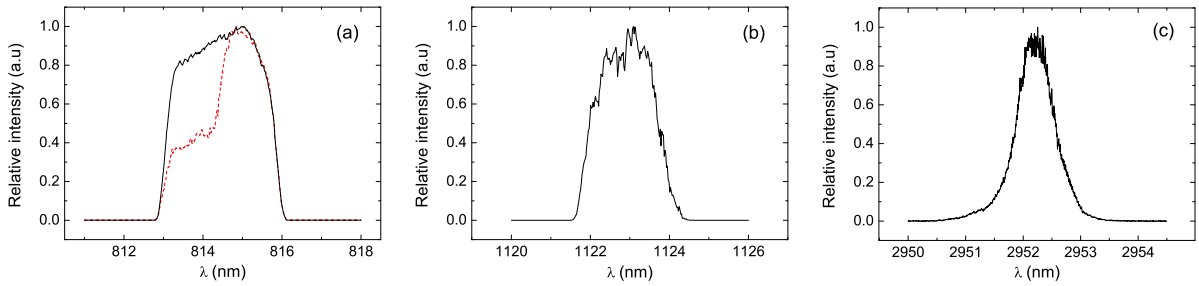

FIG. 1: Experimental spectra: Undepleted (solid line) and depleted (dashed line) pump (a). Co-propagating signal (b). Counter-propagating idler (c). The graphs show that the FWHM widths of the pump and signal are 1.21 THz and 410 GHz, respectively. The deconvoluted idler FWHM is 13 GHz.

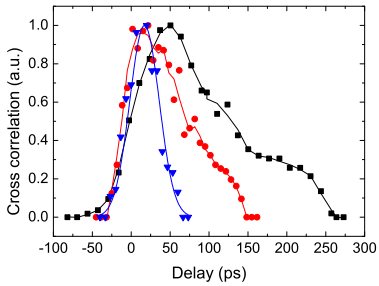

FIG. 2: Cross-correlation traces of the MOPO signal: uncompressed pulse (squares), compressor length 50 cm (circles), compressor length 86 cm (triangles).

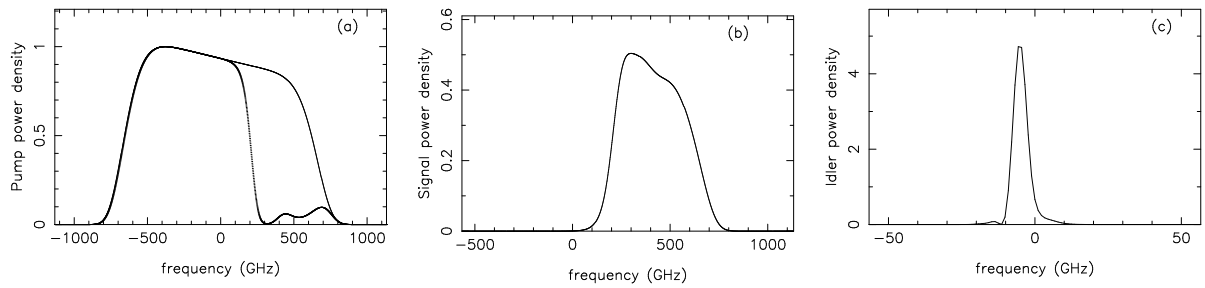

FIG. 3: Calculated spectra: Undepleted (solid line) and depleted (dotted line) pump (a). Co-propagating signal (b). Counter-propagating idler (c). The zeros on the frequency scales correspond to 814.5 nm and approximately 1125 nm and 2952 nm for the pump, signal and idler, respectively. The corresponding FWHM widths are 1.27 THz, 440 GHz and 6.5 GHz.

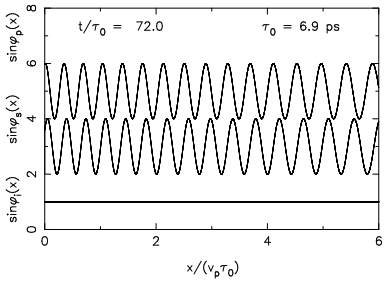

FIG. 4: Phase distribution inside the crystal for the pump, the signal (locked to the pump) and the backward idler (invariant). The x-axis is in units of $L_{nl} = v_{g,p}\tau_0 = 1$ mm.